Bistability of the Atlantic subpolar gyre in a coarse-resolution climate model

A. Levermann[1,2] and A. Born[1,2]

Received 20 August 2007; revised 12 November 2007; accepted 19 November 2007; published 22 December 2007.

[1] High resolution models indicate that the dynamics of the Nordic Seas and the subpolar gyre is crucial for deep water formation and overturning circulation in the Atlantic. During the last decades significant changes in ocean properties have been observed in this region. We show that large-scale dynamics, as captured by coarse resolution climate models, allows for a bistability of the Atlantic subpolar gyre. We suggest three positive feedbacks which yield the necessary nonlinearity for this behavior. Transitions between the two states can be triggered by small fluctuations in surface freshwater flux to the Nordic Seas, only slightly larger than natural variability presently observed in the region. **Citation:** Levermann, A., and A. Born (2007), Bistability of the Atlantic subpolar gyre in a coarse-resolution climate model, *Geophys. Res. Lett.*, *34*, L24605, doi:10.1029/2007GL031732.

1. Introduction

[2] Northern sinking of cold and saline water masses is one, possibly vulnerable, branch of the Atlantic overturning circulation [*Zickfeld et al.*, 2007]. This large scale ocean circulation influences climate regionally as well as globally [e.g., *Vellinga and Wood*, 2002; *Levermann et al.*, 2005; *Timmermann et al.*, 2005]. Most northern deep water formation occurs in the Nordic Seas in combination with strong overflows down the Greenland-Scotland ridge (GSR) and associated entrainment of surrounding water masses [*Hansen et al.*, 2004]. Recent simulations with a high resolution climate model suggest that the Atlantic inflow into the Nordic Seas is modulated significantly by the strength of the subpolar gyre (SPG) south of the GSR [*Hátún et al.*, 2005]. While surface wind stress has large influence on strength and variability of the SPG [*Curry et al.*, 1998; *Böning et al.*, 2006], part of the gyre circulation is controlled by baroclinic adjustments and therefore the density structure in the region [*Greatbatch et al.*, 1991; *Myers et al.*, 1996; *Penduff et al.*, 2000; *Eden and Willebrand*, 2001]. Measurements show a strong freshening of the region during the last four decades [*Dickson et al.*, 2002; *Curry and Mauritzen*, 2005] and satellite observation of sea surface elevation suggest a rapid reduction in SPG strength between 1992 and 2003 [*Häkkinen and Rhines*, 2004]. Thus strong changes are presently occurring within the subpolar region. In order to project its future evolution, the gap between simulations on short timescales with high resolution and those on long timescales and lower resolution needs to be overcome. Here we use the coupled climate model CLIMBER-3α which comprises interactive atmosphere, sea ice and ocean components [*Montoya et al.*, 2005]. The oceanic general circulation model is based on the MOM-3 GFDL code, with 24 variably spaced vertical levels, a coarse horizontal resolution of 3.75°, a background vertical diffusivity of $\kappa_h = 0.2 \cdot 10^{-4}$ m^2 s^{-1} and an eddy-induced tracer advection with a thickness diffusion coefficient of $\kappa_{gm} = 250$ m^2 s^{-1}. The fast computational performance of the model is achieved by application of an efficient atmospheric component POTSDAM-2 with a coarse horizontal resolution of 22.5° × 7.5°. The only flux adjustment applied in CLIMBER-3α is a wind anomaly model for the ocean wind stress.

2. Bistability and Feedbacks

[3] After standard initialization and integration for over 5000 years, the simulated SPG exhibits a stable but weak equilibrium volume transport of ~19 Sv = $19 \cdot 10^6$ m^3/s. Addition of 0.05 Sv of anomalous freshwater for 50 years to the Nordic Seas (between 63.75°N–78.75°N and 11.25°W–10°E) switches the circulation into a stronger state with ~29 Sv of SPG strength (Figure 1a) which is consistent with present day observations [*Bacon*, 1997; *Read*, 2001] and high-resolution ocean models of the region [*Treguier et al.*, 2005]. The freshwater flux was compensated in the North Pacific (between 30°N–60°N and 150°E–120°W). Further integration for 950 years shows that this second state is also stable. Application of a negative anomaly of 0.1 Sv for 50 years switches the system back to the initial state. The transitions are robust with respect to length and strength of the freshwater perturbations, to wind forcing and have been observed in different model configurations (will be shown in future publication).

[4] In our model, the bistability can be understood as follows. The SPG is at the center of three positive feedback loops which cause the nonlinear response of the system (Figure 2). First, a stronger gyre transports more tropical saline water into the subpolar region, as opposed to the Nordic Seas. This result is consistent with high-resolution model simulations which exhibit a decreased salinity transport towards the Nordic Seas when the SPG is strong [*Hátún et al.*, 2005]. Compared to a weaker gyre, less tropical waters are transported to the Nordic Seas, more of it recirculates in the SPG, making the center saltier (Figures 3b and 4b). This increases the density gradient between the gyre and the relatively light exterior (Figures 3c and 4c). Consequently sea surface elevation drops and the corresponding geostrophic response strengthens the circu-

[1]Earth System Analysis, Potsdam Institute for Climate Impact Research, Potsdam, Germany.
[2]Institute of Physics, Potsdam University, Potsdam, Germany.

0094-8276/07/2007GL031732

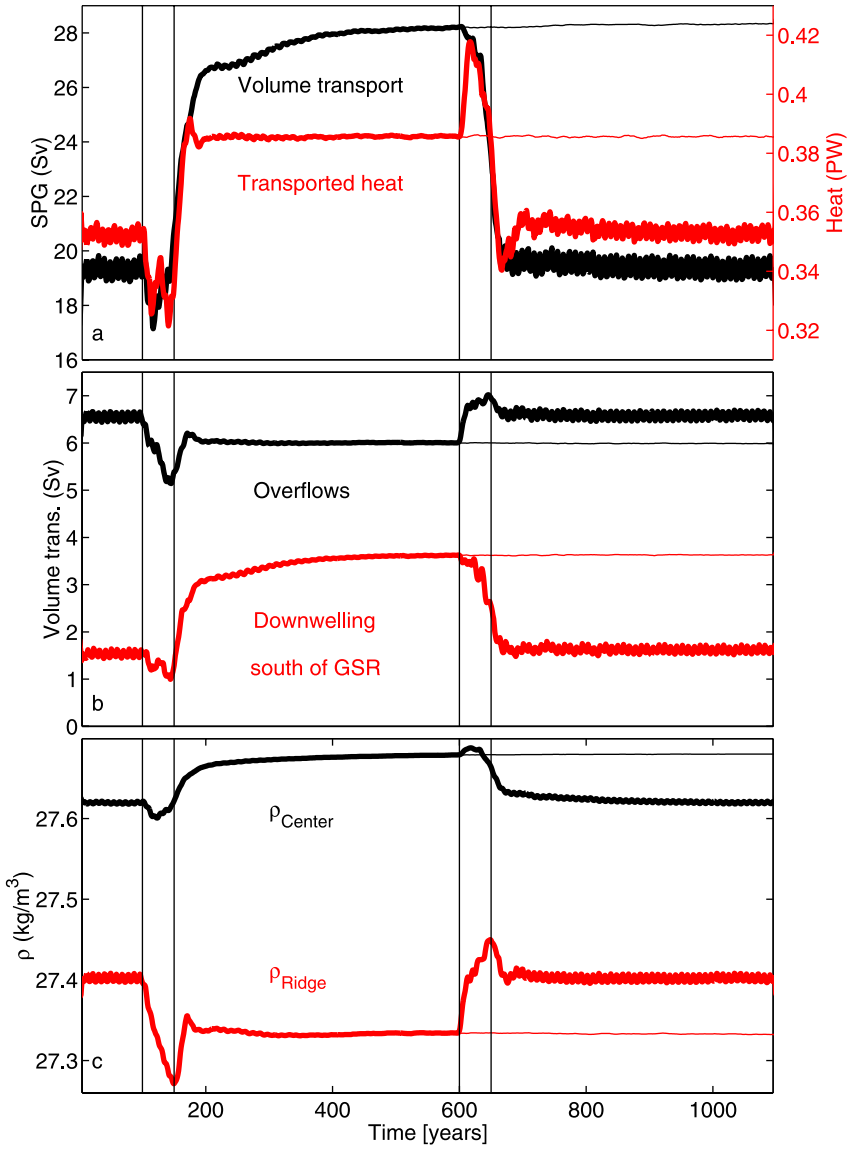

Figure 1. Time evolution of the main dynamic quantities of feedbacks from Figure 2. (a) Volume (black, left axis in Sv) and heat (red, right axis, in PW) transported by the SPG. (b) Volume transport over the GSR (black, in Sv, defined as integrated southward velocities below 500 m depth) and downwelling south of the ridge (red, in Sv, defined as difference of the zonally integrated streamfunction between 46.875°N and 54.375°N at 993 m depth). (c) Densities averaged over the upper 2000 m at the center of the SPG ρ_{Center} (black, in kg m^{-3}, averaged in (45°N, 63.75°N) × (45°W, 15°W)) and at the northern rim of the SPG at the slope of the GSR ρ_{Ridge} (red, in kg m^{-3}, averaged in (63.75°N, 67.5°N) × (45°W, 15°W)). A freshwater anomaly of 0.05 Sv (starting at year 100) for 50 years triggers a transition from the weak initial state to the stronger state. The anomalous buoyancy in the Nordic seas first reduces the overflow and therewith decreases the density south of the ridge which triggers the external feedback. The internal feedbacks amplify the effect with a time delay. Further integration for 950 years shows a stable circulation (thin lines). Application of a negative anomaly of −0.1 Sv (starting at year 600) switches the circulation back (thick lines). Thin vertical lines indicate changes in surface buoyancy forcing.

lation (internal salinity feedback). The bottom pressure is practically unchanged. Secondly, a stronger SPG results in stronger outcropping of isopycnals in the center of the gyre (Figure 4a). Therefore heat is mixed more efficiently to depth and out of the center of the SPG which results in a cooling there (Figures 3a and 4a). This again increases the core density of the gyre and therewith its strength (internal temperature feedback).

[5] In addition to these self-sustaining internal feedbacks, there exists an interaction with the flow over the GSR. A stronger SPG reduces Atlantic inflow into the Nordic Seas. More water downwells south of the GSR, less overflows the ridge (Figure 1b). As a consequence, waters at the northern rim of the gyre (south of the ridge) get lighter, because they are fed by relatively light water that is formed south of the ridge as opposed to the dense overflow waters (Figures 3c

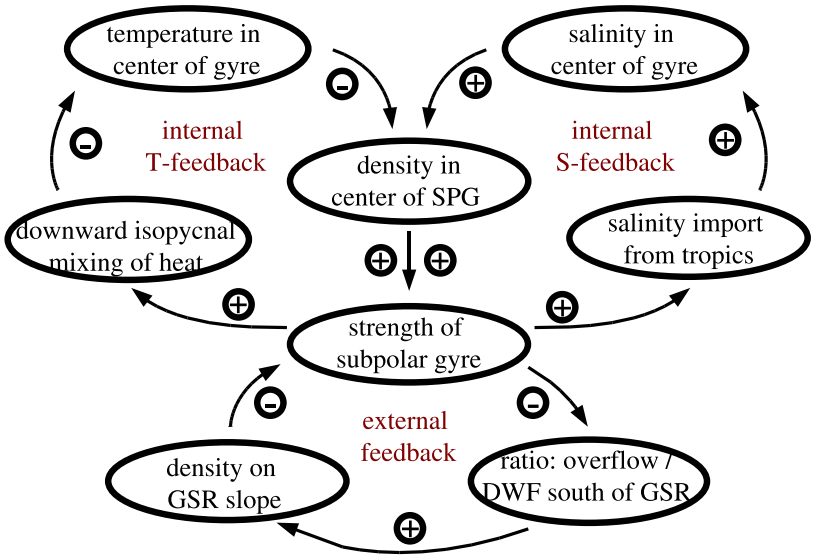

Figure 2. Three positive feedback loops yielding the bistability of the subpolar gyre in the model. In the course of the simulation the "external feedback" triggers the transition between the two states which is then dominated by the processes of the two "internal feedbacks."

and 4c). This increases the density gradient across the gyre and enhances its strength (positive external feedback).

[6] The causal chain of events in the simulations shown in Figure 1 is related to the three described feedbacks. The first application of the positive freshwater anomaly causes an immediate reduction in overflow strength less than 5 years after the freshwater perturbation (Figure 1b) which yields a rapid decline in density along the GSR, i.e. at the northern rim of the SPG ($\sim$0.12 kg/m^3 within 50 years, Figure 1c). This triggers the external positive feedback (Figure 2). The successive increase in SPG volume transport (Figure 1a) affects the two positive internal feedbacks and causes the main increase in gyre strength. The time lag of the internal feedbacks compared to the external one can be seen in the delayed response of the density at the center of the gyre, which rises only $\sim$50 years after the onset of the perturbation (Figure 1c). The negative freshwater anomaly shows the same succession of events only that the overflows are enhanced in response to the densification of the surface water and the external feedback is triggered negatively, leading to a reduction in SPG strength.

[7] The two stable states of the SPG are associated with different climate states. In contrast to previous studies [*Häkkinen*, 2001], shape and strength of the overturning does not vary between the two states (less than 0.5 Sv difference). Thus the inflow of tropical waters into the subpolar region is practically unchanged, while the circulation rearranges in the subpolar region. The increased heat transport of a stronger gyre (Figure 1a) enhances surface air temperature by up to 1.4°K south of Greenland. Sea surface elevation in the gyre follows the temporal evolution of the SPG strength and is more than 0.25 m lower in the stronger state. Sea surface elevation was previously used as an index for SPG strength [*Häkkinen*, 2001]. The rate of change reported from satellite observations for the period between 1992 and 2003 was on average about $\sim$0.2 m per decade and was associated with a strong warming within the center of the gyre [*Häkkinen and Rhines*, 2004]. The observed warming is consistent with the presented temperature feedback (Figure 2) which is associated with a decline in sea surface elevation of $\sim$0.25 m over the period of 50 years in our simulations.

3. Conclusion and Discussion

[8] We would like to emphasize that the feedback loops in Figure 2 depend exclusively on large scale properties of the circulation. Due to the coarse resolution of the model, deep water formation south of the GSR is shifted from Labrador Sea towards Irminger Sea (around 55°N and 30°W, Figure 3). Though the SPG does not exhibit the observed excursion into the Labrador Sea, the model reproduces general dynamical features of higher resolution models [*Spall*, 2005]. The main sinking occurs at the rim of the SPG while convection occurs at its center (both not shown). The heat transport from the rim to the center is at least partly due to eddy transport, parameterized following *Gent and McWilliams* [1990], as observed in the Labrador Sea [*Straneo*, 2006].

[9] Simulations with reduced surface wind stress in the North Atlantic show that the wind plays a key role for the strength of the SPG (not shown). However, it does not influence the transition between the two states, as can be seen from a simulation with prescribed surface wind stress, which shows the same behavior. Variability in wind and buoyancy flux, for example, due to the North Atlantic Oscillation are not captured by our simulations and might counteract some of the feedbacks presented here. Higher resolution model studies have to clarify which effects dominate.

[10] The representation of the overflows, which is part of the external feedback, is particularly coarse in CLIMBER-3α and we can not claim to capture the small scale physics of this flow. In fact our model suffers from the same strong dilution of water mass properties along the pathway down the GSR as other coarse resolution models [*Bailey et al.*, 2005]. For the presented feedbacks, it is merely necessary

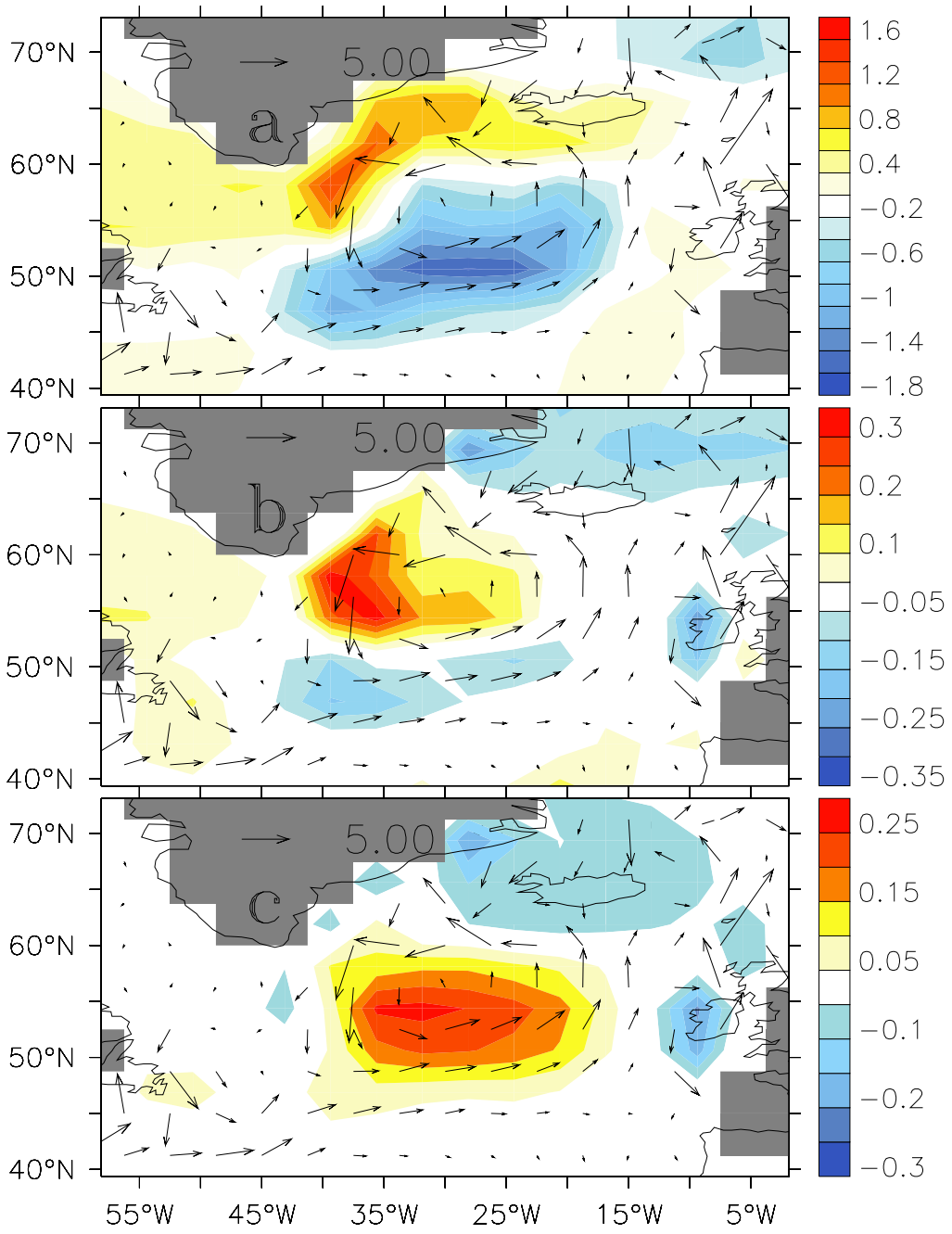

Figure 3. Difference strong minus weak SPG-state (averaged over upper 1000 m): (a) temperature (in K), (b) salinity (in psu), and (c) density (in kg m^{-3}). Vectors show vertically averaged horizontal velocities (in 10^{-2} m s^{-1}). The density at the center of the stronger SPG is enhanced both due to increased salinity and decreased temperature.

that the overflow waters are denser than the downwelling south of the ridge, which is the case in the model and observed in the ocean. In the presented simulations, downwelling south of the ridge enhances as a response to reduced northward flow into the Nordic Seas. This results partly from inertia of the flow (i.e. the tropical northward flow does not respond immediately to changes in northern convection) and partly from the fact that the overturning in CLIMBER-3α is mainly driven by surface wind stress in the Southern Ocean [*Levermann et al.*, 2007], which does not change in the course of the simulations. While at present neither observations nor high resolution model results can ultimately clarify whether this is the case, it is not necessary for the existence of the external feedback. Note that this external feedback plays a special role in the mechanism. In the Nordic Seas, changes in surface forcing are directly transported to intermediate depth south of the GSR through deep water formation and alter the density distribution there, despite the fact that water mass dilution is unrealistically strong in our coarse resolution model. If, in contrast, the forcing is changed in the subpolar region, the strong wind-driven gyre circulation at the surface dilutes the signal. As a consequence, we have not succeeded to trigger the transition between the two states by surface flux onto the SPG directly.

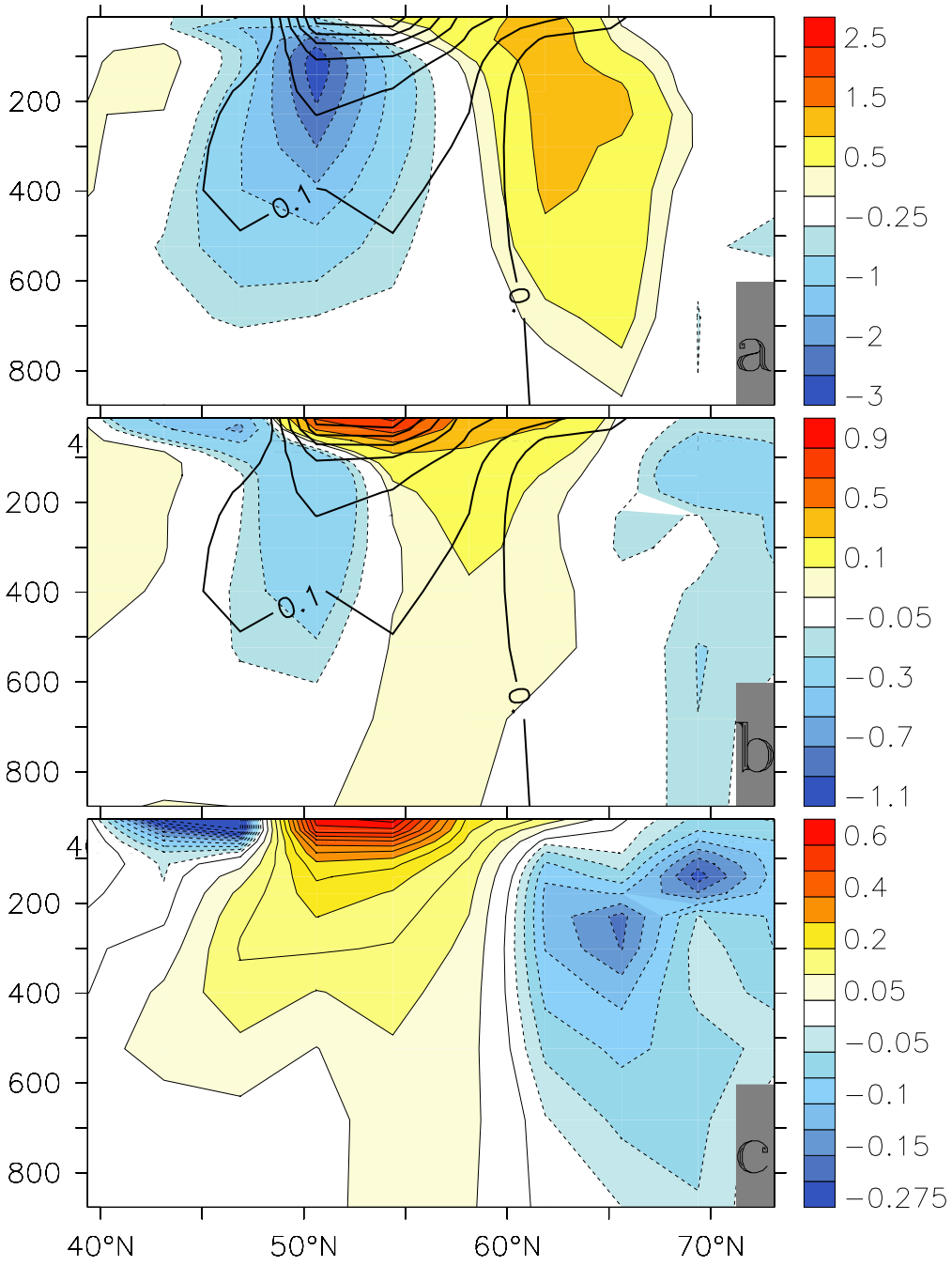

Figure 4. Difference strong minus weak SPG-state (meridional section averaged between 45°W and 15°W): (a) temperature (in K), (b) salinity (in psu), and (c) density (in kg m^{-3}). The center of the stronger SPG is denser due to reduced temperatures in the subsurface and higher salinities in the entire water column. Mainly freshening but also small reduction in temperature decreases the density along the GSR. Figures 4a and 4b also show isolines of the density difference of Figure 4c as thick lines in order to illustrate the enhanced isopycnal mixing of heat and salinity out of the center of the SPG (contour line step of 0.1 kg/m^3).

[11] Sensitivity experiments show that application of 0.05 Sv of freshwater into the Nordic Seas for 25 years is sufficient for the transition from weak to strong SPG state. The associated amount of freshwater is about four times as large as the one associated with the Great Salinity Anomaly of the 1960s [*Curry and Mauritzen*, 2005]. Integration of precipitation into the Nordic Seas from the NCEP-NCAR reanalysis reveal fluctuations from 0.09 Sv to 0.17 Sv between 1958 and 2005. The strongest persistent deviation from the long term mean of 0.13 Sv occurred between 1961 and 1970. It had a mean amplitude of about 0.02 Sv which is within the range necessary to trigger the transition. CLIMBER-3α is lacking atmospheric variability and is therefore unable to simulate these variations. For future climate, also other possible freshwater sources have to be taken into account. Climate projections for the 21st century

suggest that Greenland can contribute of the order of 0.1 Sv of surface freshwater flux [*Winguth et al.*, 2005]. Arctic runoff has been reported to increase by about 0.0025 Sv during the last 6 decades [*Peterson et al.*, 2002].

[12] This study means to present a possible mechanism for a multistability of the subpolar gyre system based on large-scale ocean circulation. Though bistability has been observed in a higher resolution model (H. Drange, personal communication, 2007), further studies with eddy-resolving models are necessary to investigate the robustness of the different feedbacks.

[13] **Acknowledgments.** We would like to thank J. Mignot and B. Marzeion for comments on an earlier draft.

References

Bacon, S. (1997), Circulation and fluxes in the North Atlantic between Greenland and Ireland, *J. Phys. Oceanogr.*, *27*, 1420–1435.

Bailey, D. A., P. B. Rhines, and S. Häkkinen (2005), Formation and pathways of North Atlantic Deep Water in a coupled ice-ocean model of the Arctic-North Atlantic Oceans, *Clim. Dyn.*, *25*, 497–516.

Böning, C., M. Scheinert, J. Dengg, A. Biastoch, and A. Funk (2006), Decadal variability of subpolar gyre transport and its reverberation in the North Atlantic overturning, *Geophys. Res. Lett.*, *33*, L21S01, doi:10.1029/2006GL026906.

Curry, R., and C. Mauritzen (2005), Dilution of the Northern North Atlantic Ocean in recent decades, *Science*, *308*, 1772–1774.

Curry, R., M. McCartney, and T. Joyce (1998), Oceanic transport of subpolar climate signals to mid-depth subtropical waters, *Nature*, *391*, 575–577.

Dickson, B., I. Yashayaev, J. Meincke, B. Turrell, S. Dye, and J. T. Holfort (2002), Rapid freshening of the deep North Altantic Ocean over the past four decades, *Nature*, *416*, 832–837.

Eden, C., and J. Willebrand (2001), Mechanism of interannual to decadal variability of the North Atlantic Circulation, *J. Clim.*, *14*, 2266–2280.

Gent, P. R., and J. C. McWilliams (1990), Isopycnal mixing in Ocean Circulation Models, *J. Phys. Oceanogr.*, *20*, 150–155.

Greatbatch, R., A. Fanning, A. Goulding, and S. Levitus (1991), A diagnosis of interpentadal circulation changes in the north Atlantic, *J. Geophys. Res.*, *96*, 22,009–22,023.

Häkkinen, S. (2001), Variability in sea surface height: A qualitative measure for the meridional overturning in the North Atlantic, *J. Geophys. Res.*, *106*, 13,837–13,848.

Häkkinen, S., and P. B. Rhines (2004), Decline of subpolar North Atlantic circulation during the 1990s, *Science*, *304*, 555–559.

Hansen, B., S. Østerhus, D. Quadfasel, and W. Turrell (2004), Already the day after tomorrow?, *Science*, *305*, 953–954.

Hátún, H., A. Sandø, H. Drange, B. Hansen, and H. Valdimarsson (2005), Influence of the Atlantic subpolar gyre on the thermohaline circulation, *Science*, *309*, 1841–1844.

Levermann, A., A. Griesel, M. Hofmann, M. Montoya, and S. Rahmstorf (2005), Dynamic sea level changes following changes in the thermohaline circulation, *Clim. Dyn.*, *24*, 347–354.

Levermann, A., J. Schewe, and M. Montoya (2007), Lack of bipolar seesaw in response to Southern Ocean wind reduction, *Geophys. Res. Lett.*, *34*, L12711, doi:10.1029/2007GL030255.

Montoya, M., A. Griesel, A. Levermann, J. Mignot, M. Hofmann, A. Ganopolski, and S. Rahmstorf (2005), The Earth System Model of Intermediate Complexity CLIMBER-3α. Part I: Description and performance for present day conditions, *Clim. Dyn.*, *25*, 237–263.

Myers, P., A. Fanning, and A. Weaver (1996), Jebar, bottom pressure torque, and gulf stream separation, *J. Phys. Oceanogr.*, *26*, 671–683.

Penduff, T., B. Barnier, and A. C. de Verdière (2000), Self-adapting open boundaries for a sigma coordinate model of the eastern North Atlantic, *J. Geophys. Res.*, *105*, 11,279–11,298.

Peterson, B. J., R. M. Holmes, J. W. McClelland, J. Vörösmarty, R. B. Lammers, A. I. Shiklomanov, I. A. Shiklomanov, and S. Rahmstorf (2002), Increasing river discharge to the Arctic Ocean, *Science*, *298*, 2171–2173.

Read, J. (2001), CONVEX-91: Water masses and circulation of the northeast Atlantic subpolar gyre, *Prog. Oceanogr.*, *48*, 461–510.

Spall, M. A. (2005), Buoyancy-forced circulations in shallow marginal seas, *J. Mar. Res.*, *63*, 729–752.

Straneo, F. (2006), Heat and freshwater transport through the central Labrador Sea, *J. Phys. Oceanogr.*, *36*, 606–628.

Timmermann, A., S. I. An, U. Krebs, and H. Goosse (2005), ENSO suppression due to weakening of the North Atlantic thermohaline circulation, *J. Clim.*, *18*, 2842–2859.

Treguier, A. M., S. Theetten, E. Chassignet, T. Penduff, R. Smith, L. Talley, J. Beismann, and C. Böning (2005), The North Atlantic Subpolar Gyre in four high-resolution models, *J. Clim.*, *35*, 757–774.

Vellinga, M., and R. A. Wood (2002), Global climatic impacts of a collapse of the Atlantic thermohaline circulation, *Clim. Change*, *54*, 251–267.

Winguth, A., U. Mikolajewicz, M. Gröger, E. Maier-Reimer, G. Schurgers, and M. Vizcaíno (2005), Centennial-scale interactions between the carbon cycle and anthropogenic climate change using a dynamic Earth system model, *Geophys. Res. Lett.*, *32*, L23714, doi:10.1029/2005GL023681.

Zickfeld, K., A. Levermann, H. M. Granger, S. Rahmstorf, T. Kuhlbrodt, and D. W. Keith (2007), Expert judgements on the response of the Atlantic Meridional Overturning Circulation to climate change, *Clim. Change*, *82*, 235–265.

A. Born and A. Levermann, Earth System Analysis, Potsdam Institute for Climate Impact Research, Telegrafenberg A62, D-14473 Potsdam, Germany. (anders.levermann@pik-potsdam.de)